

## Superconductor-Insulator Transition in a Non-Fermi Liquid

A. L. Chudnovskiy<sup>1</sup> and Alex Kamenev<sup>2,3</sup>

<sup>1</sup>*Institut für Theoretische Physik, Universität Hamburg, Notkestraße 9, D-22607 Hamburg, Germany*

<sup>2</sup>*School of Physics and Astronomy, University of Minnesota, Minneapolis, Minnesota 55455, USA*

<sup>3</sup>*William I. Fine Theoretical Physics Institute, University of Minnesota, Minneapolis, Minnesota 55455, USA*



(Received 27 July 2022; accepted 7 December 2022; published 22 December 2022)

We present a model of a strongly correlated system with a non-Fermi liquid high temperature phase. Its ground state undergoes an insulator to superconductor quantum phase transition (QPT) as a function of a pairing interaction strength. Both the insulator and the superconductor are originating from the same interaction mechanism. The resistivity in the insulating phase exhibits the activation behavior with the activation energy, which goes to zero at the QPT. This leads to a wide quantum critical regime with an algebraic temperature dependence of the resistivity. Upon raising the temperature in the superconducting phase, the model exhibits a finite temperature phase transition to a Bose metal phase, which separates the superconductor from the non-Fermi liquid metal.

DOI: 10.1103/PhysRevLett.129.266601

Quantum phase transition between the superconducting and insulating phases is observed in a variety of experimental systems, notably high- $T_c$  materials [1–5], dirty superconducting films [6–11], and Josephson junction arrays [12–14]. One concept of the insulating phase is that of a system with a finite local superconducting order, but without the long-range phase coherence [15–20]. It presumes that Cooper pairs are dominant charge carriers for the electric transport not only in the superconducting but also in the insulating or metallic phases. Remarkably, the high-temperature behavior of many of these systems is characterized as a strange metal with the linear in temperature resistivity.

Here we investigate a rather simple model, where the non-Fermi liquid strange metal state undergoes the superconducting instability upon lowering the temperature. The origin of the superconductivity is in a certain pairing mechanism [21–27], which we do not discuss in detail and introduce phenomenologically as a negative Hubbard  $U$  [28]. The locality of the pairing interaction distinguishes our model from other scenarios of the Sachdev-Ye-Kitaev (SYK) superconductivity. We show that the *same* local pairing mechanism is responsible for the existence of the insulating phase. The latter is separated from the superconductor by a quantum phase transition (QPT) at a critical value of the pairing strength  $U_c$ ; see Fig. 1. Within the insulating phase the low temperature resistivity exhibits the activation behavior,  $R \propto \exp\{\epsilon_1/T\}$ , with an activation energy  $\epsilon_1(U)$ . Importantly, the activation energy tends to zero upon approaching the insulator to superconductor QPT,  $\epsilon_1(U) \rightarrow 0$  when  $U \rightarrow U_c - 0$ . This gives rise to a wide quantum critical regime above the QPT, which manifests itself as an insulator with the algebraically divergent resistivity. Yet the high-temperature resistivity

in both the insulating and the superconducting phases exhibits linear behavior with the temperature  $R \propto T$ , attributed to the parent non-Fermi liquid state.

The model consists of an array of SYK [29,30] grains, coupled through the single particle tunneling. Each grain contains  $N \gg 1$  degenerate orbitals, with random four-fermion interactions. This model was thoroughly investigated in Refs. [31–36], where it was shown that its high temperature phase is a non-Fermi liquid metal with the linear in temperature resistivity. To facilitate superconductivity we introduce a local attractive interactions between electrons with opposite spins. The corresponding Hamiltonian is written as the sum of the intragrain SYK +  $U$  model and the intergrain tunneling

$$H = \sum_r H_{\text{SYK}+U}^{(r)} + \sum_{\langle r, r' \rangle} H_{\text{t}}^{(r, r')}. \quad (1)$$

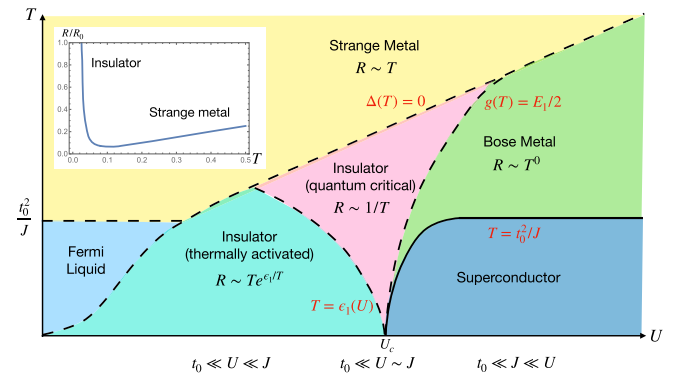


FIG. 1. Sketch of the phase diagram of the SYK + U array. Inset: temperature dependence of the resistivity in the insulating phase.

Here the first term describes the set of isolated SYK +  $U$  grains labeled by  $r$ ,

$$H_{\text{SYK}+U}^{(r)} = \sum_{ijkl;\sigma\sigma'}^N J_{ijkl}^{(r)} c_{r,i\sigma}^\dagger c_{r,j\sigma'}^\dagger c_{r,k\sigma'} c_{r,l\sigma} - U \sum_i^N c_{r,i\uparrow}^\dagger c_{r,i\downarrow}^\dagger c_{r,i\downarrow} c_{r,i\uparrow}, \quad (2)$$

where  $J_{ijkl}^{(r)}$  is a real tensor with the following symmetry properties:  $J_{ij;kl}^{(r)} = -J_{ji;kl}^{(r)} = -J_{ij;lk}^{(r)} = J_{lk;ji}^{(r)}$ . The nonzero elements must have all four indexes  $i, j, k, l$  distinct. Up to these symmetries, the matrix elements  $J_{ijkl}^{(r)}$  are assumed to be real independent random variables (uncorrelated between different grains), drawn from the Gaussian distribution with the zero mean,  $\langle J_{ijkl}^{(r)} \rangle = 0$ , and the variance  $\langle (J_{ijkl}^{(r)})^2 \rangle = J^2/(4N)^3$ . The last term in Eq. (2) is the attractive Hubbard interaction, facilitating local on-orbital electron pairing.

The spin conserving intergrain tunneling is governed by the Hamiltonian

$$H_t^{(r,r')} = \sum_{ij;\sigma}^N t_{ij}^{(r,r')} c_{ri\sigma}^+ c_{r'i\sigma}^-, \quad (3)$$

where  $t_{ij}^{(r,r')}$  are real Gaussian variables with zero mean and  $\langle (t_{ij}^{(r,r')})^2 \rangle = t_0^2/N$ . Here  $r, r'$  denotes nearest neighbor positions of SYK +  $U$  grains within the array, and  $i, j = 1, \dots, N$  denote orbital labels within each grain. Throughout this Letter, we assume the intergrain tunneling to be much less than the SYK coupling constant,  $t_0 \ll J$ .

Before tackling the array geometry, let us briefly recall the physics of a single SYK +  $U$  grain, as described by Eq. (2) [21,28]. Its large- $N$  mean-field analysis results in the set of equations for the normal  $G$  and anomalous  $F$  Green functions, the corresponding self-energies  $\Sigma, \Xi$ , and the self-consistent equation for the local (on-orbital) order parameter,  $\Delta$ :

$$G(\omega_n) = \frac{-i\omega_n + \Sigma(\omega_n)}{[\omega_n + i\Sigma(\omega_n)]^2 + [\bar{\Xi}(\omega_n) + \bar{\Delta}][\Xi(\omega_n) + \Delta]}, \quad (4)$$

$$F(\omega_n) = \frac{-[\Delta + \Xi(\omega_n)]}{[\omega_n + i\Sigma(\omega_n)]^2 + [\bar{\Xi}(\omega_n) + \bar{\Delta}][\Xi(\omega_n) + \Delta]}, \quad (5)$$

$$\Sigma_{\tau\tau'} = \frac{J^2}{32} G_{\tau\tau'}^3, \quad \Xi_{\tau\tau'} = -\frac{J^2}{32} \bar{F}_{\tau\tau'} F_{\tau\tau'}^2, \quad (6)$$

$$\Delta = -UT \sum_{\omega_n} F(\omega_n) = -UF_{\tau\tau}. \quad (7)$$

The solution of Eqs. (4)–(7) shows that at  $T = 0$  there is a finite local pairing amplitude  $\Delta(U)$  for any however small Hubbard  $U > 0$ . In particular, in the weak-coupling BCS limit  $U \ll J$ , it is given by  $\Delta \sim J \exp\{-\sqrt{\pi}J/(8\sqrt{2}U)\}$ . The solution of equations (4)–(7) also implies the hard energy gap,  $\sim \Delta^2/J$ , in the *single-particle* density of states (DOS).

The mean-field treatment fails to account for fluctuations of the low-energy degrees of freedom represented by phases of local pairing amplitudes,  $\langle c_{j\downarrow} c_{j\uparrow} \rangle = \Delta e^{i\phi_j}$ , with  $j = 1, \dots, N$ . The dynamics of these phases is governed by an effective Hamiltonian

$$H_K = -E_1 \sum_i^N \frac{\partial^2}{\partial \phi_i^2} - \frac{g}{N} \sum_{i < j}^N \cos(\phi_i - \phi_j), \quad (8)$$

which represents the quantum version of the classical Kuramoto model of oscillator's synchronization [37–47]. Here  $E_1 \approx 0.52J$  [48] and  $g(U) \approx 16\Delta^2(U)/J$  [28]. The quantum Kuramoto model [Eq. (8)] exhibits a second order transition [28] between the nonsynchronized and synchronized ground states at the critical coupling  $g_c = E_1/2$ . The corresponding global (within the grain) order parameter is given by the ground state expectation value of the phase exponents  $\langle \sum_j^N e^{i\phi_j} \rangle$ . For  $g > g_c$ , it acquires a finite value, and the ground state of the Hamiltonian (8) possesses the off-diagonal long-range order. Hence the grain is superconducting. For  $g < g_c$ , the orbital-specific superconducting phases are nonsynchronized. Therefore, despite having a finite on-orbital order parameter  $\Delta$ , the ground state of the grain does not exhibit the long-range order and the superconductivity. Given that the single-particle DOS is gapped, this leads to an insulating ground state.

This physics may be read off the correlation function of the order parameter  $\mathcal{D}_0(\tau - \tau') = (1/N) \sum_{i,j=1}^N \langle e^{i\phi_i(\tau)} e^{-i\phi_j(\tau')} \rangle$ . Its calculation in the nonsynchronized (insulating) phase, detailed in the Supplemental Material [49], results in

$$\mathcal{D}_0(\omega_m) = \frac{2E_1}{\omega_m^2 + \epsilon_1^2}, \quad (9)$$

where

$$\epsilon_1(U) = \sqrt{E_1[E_1 - 2g(U)]}, \quad (10)$$

and  $\omega_m = 2\pi mT$  is bosonic Matsubara frequency. The correlation function Eq. (9) coincides with the Green function of a bosonic mode with the energy  $\epsilon_1(U)$ . The critical pairing strength  $g_c = g(U_c)$  is found from the condition  $\epsilon_1(U) = 0$ , as it indicates an instability of the nonsynchronized phase toward a state with a nonzero global order parameter. The single mode at the energy  $\epsilon_1$  determines the whole critical behavior of the quantum Kuramoto model. The associated timescale  $1/\epsilon_1 \sim |g - g_c|^{-\nu}$  diverges at  $g_c = E_1/2$

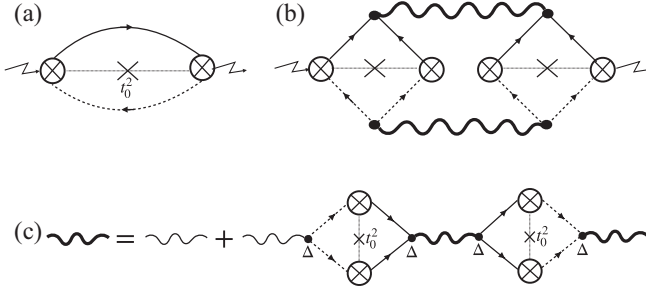


FIG. 2. (a) One-particle normal conductivity, (b) pair conductivity, and (c) Dyson equation for the order parameter propagator. Thin and bold wavy lines denote the bare, Eq. (9), and dressed in-grain order parameter propagator; solid and dashed lines denote the one-particle Green functions in different SYK grains. Vertices are given by tunneling amplitudes, and solid dots denote the superconducting amplitude,  $\Delta$ . Notice that the local self-energy, (c), involves tunneling of the pair out and back in the selected grain.

indicating a continuous phase transition with critical exponents  $z\nu = 1/2$ . The order parameter defined as the average  $(1/N) \sum_{i>j}^N \langle \cos(\phi_i - \phi_j) \rangle \propto (g - g_c)^{1/2}$  grows continuously as  $g$  exceeds the critical value [28].

The fact that the fluctuations of the order parameter exhibit a single resonant mode is a peculiarity of the Kuramoto model [Eq. (8)] with its all-to-all identical interactions. In more generic models there is a continuum of excitations. For example, substituting  $g \rightarrow g_{ij}$  in Eq. (8) and thinking of  $g_{ij}$  as a connectivity matrix on some lattice or a graph, one finds a band of Josephson plasmons [18,50,51]. The important invariant feature, however, is that such a band is gapped from the ground state in the nonsynchronized phase, while the gap closing marks QPT to the globally ordered (superconducting) phase.

Having summarized the behavior of a single SYK +  $U$  grain, we turn now to our main subject—the array of such grains. We start from the insulating phase,  $U < U_c$ . Because of the Kuramoto phase desynchronization, the supercurrent between the grains is absent. In the lowest (second) order in the tunneling amplitude,  $t_{ij}^{(r,r')}$ , the normal conductivity is given by the diagram in Fig. 2(a). The corresponding normal Green functions in two neighboring grains are given by Eq. (4). Since the DOS is gapped with the gap  $\Delta^2/J$ , this contribution to the conductivity is exponentially suppressed with a factor  $\exp\{-\Delta^2/JT\}$ . Because the orbital pairing amplitude  $\Delta$  is finite in the vicinity of the QPT, the single particle transport is strongly suppressed.

This is not the case *vis-a-vis* transport of the pairs. The latter appears in the fourth order in the tunneling amplitude and is given by the diagram in Fig. 2(b), which is close in spirit to the Aslamazov-Larkin paraconductivity [52–55]. The bold wavy lines there are propagators of the order parameter. Its bare form, given by Eq. (9), is dressed by a bosonic self-energy, as shown in Fig. 2(c). Its imaginary

part,  $\gamma$ , accounts for a finite lifetime of a pair inside a grain due to tunneling to neighboring grains (the real part leads to a shift of the resonant energy  $\epsilon_1$ , which is of lesser interest). Within our model  $\gamma$  is found from the self-consistent solution as  $\gamma \sim \sqrt{Z}E_JE_1/\epsilon_1$  for  $\epsilon_1 > Z^{1/4}\sqrt{E_JE_1}$ , and  $\gamma \sim Z^{1/4}\sqrt{E_JE_1}$  for  $\epsilon_1 < Z^{1/4}\sqrt{E_JE_1}$  (for details see the Supplemental Material [49]). Here  $Z$  is the coordination number of the array, and the pair tunneling amplitude,  $E_J \sim t_0^2/J$ , given by the box in Figs. 2(b) and 2(c), represents the Josephson energy of the array (see the Supplemental Material for detailed calculations [49]). We note in passing that  $\gamma$  may include other mechanisms of the bosonic mode broadening, such as circuit noise or phonons. The intermediate formulas below account for those effects.

The dressed retarded (advanced) propagators are given by  $\mathcal{D}^{R(A)}(\omega) = \mathcal{D}_0(i\omega \mp \gamma)$ . Calculation of the diagram (b) in Fig. 2 [49] results in the pair conductivity of the form

$$\sigma = -\frac{(2e)^2}{h} E_J^2 \int_{-\infty}^{\infty} \frac{d\omega}{8T \sinh^2(\frac{\omega}{2T})} (\mathcal{D}^R(\omega) - \mathcal{D}^A(\omega))^2. \quad (11)$$

In the limit  $T, \gamma < \epsilon_1$ , one finds with the help of Eq. (9)

$$\sigma = \frac{(2e)^2}{h} \frac{8\pi E_J^2 E_1^2}{\epsilon_1^2 T \gamma} e^{-\epsilon_1/T} \sim \frac{(2e)^2}{h} \frac{t_0^2}{\epsilon_1 T} e^{-\epsilon_1/T}. \quad (12)$$

Therefore the pair transport in the insulating state of the array exhibits the activation dependence on the temperature. The corresponding activation exponent,  $\epsilon_1(U)$  [Eq. (10)], is given by the gap in the fluctuation spectrum of the global order parameter. This gap goes to zero at the insulator to superconductor QPT, and therefore so does the activation energy of the pair conductivity. This behavior should be contrasted with the single particle conductivity [Fig. 2(a)]. The latter is also activational, but its activation energy remains finite across the QPT. As a result, the pair tunneling is the dominant transport mechanism close to the QPT. (Notice that, if the pair tunneling is the dominant mechanism of the mode broadening  $\gamma$ , both the single-particle and the pair conductivity are proportional to  $t_0^2$ .)

Equation (12) is not applicable in the quantum critical regime where  $T > \epsilon_1$ . In this case Eq. (11) yields conductivity which is a power law in temperature

$$\sigma \propto \frac{e^2 E_J^2 E_1^2 T}{h \gamma^6} \times \begin{cases} T & \text{for } T < \gamma, \\ \gamma & \text{for } T > \gamma. \end{cases} \quad (13)$$

These power laws represent Gaussian exponents of the QPT. We do not attempt here to discuss if fluctuation corrections affect the critical exponents. The quantum critical regime extends above the  $T = 0$  QPT point (Fig. 1), flanked by the lines  $T = \epsilon_1(U, T)$  on the left and  $\epsilon_1(U, T) = 0$  on the right. The insulating phase crosses

over into the SYK strange metal phase with the linear in  $T$  resistivity, at a temperature where the mean-field local pairing amplitude disappears  $\Delta(T) = 0$ . This temperature marks closing the gap in the single-particle spectrum due to the meltdown of the preformed Cooper pairs.

The insulating phase with a gap in the single-particle spectrum along with the preformed pairs and strong phase fluctuations between the pairs on different orbitals may be considered as a model of the pseudogap state [19,20,56–63], capturing for the antinodal part of the dispersion in d-wave superconductors. The SYK physics stems from the fact that the interaction energy between these orbitals is larger than their kinetic energy dispersion. In the array geometry it naturally leads to the linear in temperature resistivity at high enough temperature [31]. This is a particular case of the recently developed theory of the Plankian metal, which emerges as the high-temperature phase of a conducting system without coherent quasiparticles [31–36,64–66]. At the same time, the strange metal theory is infrared incomplete. That is, there are many possible scenarios of the low-temperature phases that have a strange metal as their high-temperature limit [67–71]. The local orbital pairing phenomenology leads to the quantum Kuramoto model as its low-energy effective theory. The latter yields the insulating pseudogap phase with the activation resistivity and activation energy vanishing at the insulator to superconductor QPT.

We turn now to the superconducting side of the QPT. Here the ground state of each isolated grain is superconducting. The grains thus form the Josephson junction array with the intergrain Josephson energy  $E_J \sim t_0^2/J$ . Since the individual phases of  $N$  orbitals within each grain are locked  $\phi_i^{(r)} = \phi^{(r)}$ , the grain's charging energy is  $E_C = E_1/N \ll E_J$ . In other words, the effective electric capacitance of the whole grain is  $N$  times larger than the quantum capacitance of the single orbital.

By raising the temperature, the array undergoes the classical phase transition to the incoherent state at the critical temperature of the order of the Josephson energy  $E_J$ . At temperatures higher than the Josephson energy but still below the superconducting energy gap, the phase coherence between the grains in the array is lost, while each grain in the array remains superconducting. Therefore the single-particle transport is suppressed, and the normal current is carried by incoherent Cooper pairs. It is thus denoted as Bose metal in Fig. 1.

In the Bose metal regime the conductivity of the array can be calculated from the conductivity of a single junction with simple circuit theory rules. We thus evaluate the conductivity of one junction, considering the rest of the array as an effective dissipative medium. Within this approach an escape of a Cooper pair from a grain through  $(Z - 1)$  other junctions provides a mechanism for the loss of the phase coherence across the junction of interest. The single Josephson junction is governed by the action

$$S_{JJ} = \int dt \left\{ \frac{\dot{\phi}^2}{2E_C} + E_J \cos(\phi) \right\}. \quad (14)$$

The resulting equation of motion  $\ddot{\phi} = E_C E_J \sin(\phi)$  describes dynamics of the superconducting phase of an isolated junction. For a junction embedded in the incoherent array, the equation of motion above is amended with the relaxation term and the corresponding Langevin noise

$$\frac{(2e)^2}{E_C} \ddot{\phi} + \sigma \dot{\phi} = (2e)^2 E_J \sin(\phi) + \xi(t). \quad (15)$$

The dissipation coefficient  $\sigma$  and the Langevin noise  $\xi$  are tied by the fluctuation-dissipation relation

$$\langle \xi(t) \xi(t') \rangle = 2\sigma T \delta(t - t'). \quad (16)$$

Consequently  $\sigma$  is identified with the Ohmic conductivity of the junction, which is in turn related to the circuit  $RC$  relaxation rate  $\gamma$  as  $\sigma = (2e)^2 \gamma / E_C$ . The  $RC$  relaxation rate is given by a pair escape into the rest of the array evaluated in the Supplemental Material [49] as  $\gamma = \sqrt{Z} E_J$ . With this we obtain for the conductivity of the Bose metal

$$\sigma \propto E_J / E_C \sim N \frac{t_0^2}{J^2}. \quad (17)$$

Parametrically it is the same as conductivity in the low temperature,  $T < t_0^2/J$ , Fermi liquid regime of the normal SYK array [31]. The physics, however, is very different, and the Bose metal appears at higher temperature  $T \gtrsim E_J \approx t_0^2/J$  and extends up to the in-grain critical temperature. The latter is determined by the condition  $g(T) = 16\Delta^2(U, T)/J = E_1/2$ , where the Kuramoto synchronization within the grain is lost. At higher temperature the array enters the quantum critical region described above; see Eq. (13) and Fig. 1. We note that the physical pictures of the Bose metal and the insulating phases are very similar, both consisting of incoherent Cooper pairs. In case of the insulator, they are incoherent between the sites of the same grain. In the case of Bose metal there is a coherence within the grain, but different grains are incoherent. At a finite temperature the distinction is immaterial and thus there is not any finite  $T$  transition between the insulator and Bose metal—rather a crossover, which is marked by different temperature dependencies of the resistivity: constant in the Bose metal vs rising at decreasing temperature in the insulator phase. The ground states are very different, though. In the case of the Bose metal, the ground state is superconducting, while it is insulating in the other phase.

In conclusion, we proposed an array of SYK +  $U$  grains as a microscopic model that reproduces some crucial parts of the high- $T_c$  phase diagram. Despite simplicity of its Hamiltonian, the model exhibits a rather rich phenomenology. At zero temperature it features QPT between the

insulating and the superconducting states, both induced by the Hubbard  $U$ . The insulating phase reminds the pseudogap physics of preformed incoherent Cooper pairs, described by the quantum Kuramoto picture. The low-temperature resistivity here obeys the Arrhenius law with the activation energy, which smoothly goes to zero approaching the transition. At yet a higher temperature the Cooper pairs melt giving way to a non-Fermi liquid metal with the linear in temperature resistivity. These features qualitatively agree with a nonmonotonous temperature dependence of resistance in the pseudogap phase observed in several experiments [4,72,73]. On the superconducting side of the transition, upon elevating temperature, the system goes into the Bose metal and eventually again to the non-Fermi liquid metal. The latter phenomenology is relevant for Josephson arrays [14] and for other systems featuring superconductor-insulator transition, such as disordered superconducting films, where the transport of Cooper pairs provides the dominant charge transport channel [7,9,74,75].

We are grateful to A. Chubukov, L. Glazman, A. Goldman, C. Marcus, and A. Schnirman for useful discussions. A. K. was supported by the NSF Grant No. DMR-2037654.

- [1] D. J. Scalapino, *Rev. Mod. Phys.* **84**, 1383 (2012).
- [2] Y. Cui, S. Wu, Q. Zhu, G. Xiao, B. Liu, J. Wu, G. Cao, and Z. Ren, *npj Quantum Mater.* **6**, 74 (2021).
- [3] Q. Guo and B. Noheda, *npj Quantum Mater.* **6**, 72 (2021).
- [4] N. Doiron-Leyraud, P. Auban-Senzier, S. René de Cotret, C. Bourbonnais, D. Jérôme, K. Bechgaard, and L. Taillefer, *Phys. Rev. B* **80**, 214531 (2009).
- [5] T. Timusk and B. Statt, *Rep. Prog. Phys.* **62**, 61 (1999).
- [6] A. M. Goldman and N. Marković, *Phys. Today* **51**, No. 11, 39 (1998).
- [7] H. M. Jaeger, D. B. Haviland, B. G. Orr, and A. M. Goldman, *Phys. Rev. B* **40**, 182 (1989).
- [8] D. B. Haviland, Y. Liu, and A. M. Goldman, *Phys. Rev. Lett.* **62**, 2180 (1989).
- [9] A. Kapitulnik, S. A. Kivelson, and B. Spivak, *Rev. Mod. Phys.* **91**, 011002 (2019).
- [10] N. P. Breznay, M. A. Steiner, S. A. Kivelson, and A. Kapitulnik, *Proc. Natl. Acad. Sci. U.S.A.* **113**, 280 (2016).
- [11] U. S. Pracht, N. Bachar, L. Benfatto, G. Deutscher, E. Farber, M. Dressel, and M. Scheffler, *Phys. Rev. B* **93**, 100503(R) (2016).
- [12] L. J. Geerligs, M. Peters, L. E. M. de Groot, A. Verbruggen, and J. E. Mooij, *Phys. Rev. Lett.* **63**, 326 (1989).
- [13] R. A. Ferrell and B. Mirhashem, *Phys. Rev. Lett.* **63**, 1753 (1989).
- [14] C. G. L. Böttcher, F. Nichele, M. Kjaergaard, H. J. Suominen, J. Shabani, C. J. Palmstrøm, and C. M. Marcus, *Nat. Phys.* **14**, 1138 (2018).
- [15] E. Šimánek, *Phys. Rev. B* **22**, 459 (1980).
- [16] E. Šimánek, *Phys. Rev. Lett.* **45**, 1442 (1980).
- [17] K. Efetov, *Sov. Phys. JETP* **51**, 1015 (1980).
- [18] S. Doniach, *Phys. Rev. B* **24**, 5063 (1981).
- [19] T. Dubouchet, B. Sacépé, J. Seidemann, D. Shahar, M. Sanquer, and C. Chapelier, *Nat. Phys.* **15**, 233 (2019).
- [20] T. Kondo, R. Khasanov, T. Takeuchi, J. Schmalian, and A. Kaminski, *Nature (London)* **457**, 296 (2009).
- [21] A. A. Patel, M. J. Lawler, and E.-A. Kim, *Phys. Rev. Lett.* **121**, 187001 (2018).
- [22] I. Esterlis and J. Schmalian, *Phys. Rev. B* **100**, 115132 (2019).
- [23] D. Chowdhury and E. Berg, *Phys. Rev. Res.* **2**, 013301 (2020).
- [24] D. Hauck, M. J. Klug, I. Esterlis, and J. Schmalian, *Ann. Phys. (Amsterdam)* **417**, 168120 (2020).
- [25] E. Lantagne-Hurtubise, V. Pathak, S. Sahoo, and M. Franz, *Phys. Rev. B* **104**, L020509 (2021).
- [26] L. Classen and A. Chubukov, *Phys. Rev. B* **104**, 125120 (2021).
- [27] G.-A. Inkof, K. Schalm, and J. Schmalian, *npj Quantum Mater.* **7**, 56 (2022).
- [28] H. Wang, A. L. Chudnovskiy, A. Gorsky, and A. Kamenev, *Phys. Rev. Res.* **2**, 033025 (2020).
- [29] S. Sachdev and J. Ye, *Phys. Rev. Lett.* **70**, 3339 (1993).
- [30] A. Kitaev, A simple model of quantum holography, <http://online.kitp.ucsb.edu/online/entangled15/kitaev/> and <http://online.kitp.ucsb.edu/online/entangled15/kitaev2/> (7 April 2015 and 27 May 2015).
- [31] X.-Y. Song, C.-M. Jian, and L. Balents, *Phys. Rev. Lett.* **119**, 216601 (2017).
- [32] A. A. Patel and S. Sachdev, *Phys. Rev. Lett.* **123**, 066601 (2019).
- [33] D. Chowdhury, A. Georges, O. Parcollet, and S. Sachdev, *Rev. Mod. Phys.* **94**, 035004 (2022).
- [34] A. A. Patel, H. Guo, I. Esterlis, and S. Sachdev, [arXiv: 2203.04990](https://arxiv.org/abs/2203.04990).
- [35] A. A. Patel, J. McGreevy, D. P. Arovas, and S. Sachdev, *Phys. Rev. X* **8**, 021049 (2018).
- [36] D. Chowdhury, Y. Werman, E. Berg, and T. Senthil, *Phys. Rev. X* **8**, 031024 (2018).
- [37] Y. Kuramoto, in *International Symposium on Mathematical Problems in Theoretical Physics*, edited by H. Araki (Springer, New York, 1975), p. 420.
- [38] J. A. Acebrón, L. L. Bonilla, C. J. P. Vicente, F. Ritort, and R. Spigler, *Rev. Mod. Phys.* **77**, 137 (2005).
- [39] F. Dörfler, M. Chertkov, and F. Bullo, *Proc. Natl. Acad. Sci. U.S.A.* **110**, 2005 (2013).
- [40] H. Daido, *Phys. Rev. Lett.* **68**, 1073 (1992).
- [41] K. Wiesenfeld, P. Colet, and S. H. Strogatz, *Phys. Rev. E* **57**, 1563 (1998).
- [42] D. Witthaut, S. Wimberger, R. Burioni, and M. Timme, *Nat. Commun.* **8**, 14829 (2017).
- [43] R. M. D’Souza, J. Gómez-Gardeñes, J. Nagler, and A. Arenas, *Adv. Phys.* **68**, 123 (2019).
- [44] S. H. Strogatz, *Physica (Amsterdam)* **143D**, 1 (2000).
- [45] S. Boccaletti, G. Bianconi, R. Criado, C. I. Del Genio, J. Gómez-Gardeñes, M. Romance, I. Sendina-Nadal, Z. Wang, and M. Zanin, *Phys. Rep.* **544**, 1 (2014).
- [46] J. Gómez-Gardeñes, Y. Moreno, and A. Arenas, *Phys. Rev. E* **75**, 066106 (2007).
- [47] A. Arenas, A. Díaz-Guilera, and C. J. Pérez-Vicente, *Physica (Amsterdam)* **224D**, 27 (2006).

[48] Y. Gu, A. Kitaev, S. Sachdev, and G. Tarnopolsky, *J. High Energy Phys.* 02 (2020) 157.

[49] See Supplemental Material at <http://link.aps.org/supplemental/10.1103/PhysRevLett.129.266601> for detailed derivations.

[50] A. van Otterlo, K.-H. Wagenblast, R. Fazio, and G. Schön, *Phys. Rev. B* **48**, 3316 (1993).

[51] S. Chakravarty, G.-L. Ingold, S. Kivelson, and A. Luther, *Phys. Rev. Lett.* **56**, 2303 (1986).

[52] L. Aslamasov and A. Larkin, *Sov. Phys. Solid State* **10**, 875 (1968).

[53] L. Aslamasov and A. Larkin, *Phys. Lett. A* **26**, 238 (1968).

[54] A. Larkin and A. Varlamov, *Theory of Fluctuations in Superconductors*, International Series of Monographs on Physics Vol. 127 (Oxford University Press, New York, 2005).

[55] I. Poboko and M. Feigel'man, *Phys. Rev. B* **97**, 014506 (2018).

[56] V. J. Emery and S. A. Kivelson, *Nature (London)* **374**, 434 (1995).

[57] J. Corson, R. Mallozzi, J. Orenstein, J. N. Eckstein, and I. Bozovic, *Nature (London)* **398**, 221 (1999).

[58] U. Chatterjee, D. Ai, J. Zhao, S. Rosenkranz, A. Kaminski, H. Raffy, Z. Li, K. Kadowaki, M. Randeria, M. R. Norman, and J. C. Campuzano, *Proc. Natl. Acad. Sci. U.S.A.* **108**, 9346 (2011).

[59] B. Keimer, S. A. Kivelson, M. R. Norman, S. Uchida, and J. Zaanen, *Nature (London)* **518**, 179 (2015).

[60] Z. Dai, T. Senthil, and P. A. Lee, *Phys. Rev. B* **101**, 064502 (2020).

[61] W.-L. Tu and T.-K. Lee, *Sci. Rep.* **9**, 1719 (2019).

[62] J. S. Hofmann, E. Berg, and D. Chowdhury, *Phys. Rev. B* **102**, 201112(R) (2020).

[63] P. A. Lee, *Phys. Rev. X* **4**, 031017 (2014).

[64] H. Guo, Y. Gu, and S. Sachdev, *Phys. Rev. B* **100**, 045140 (2019).

[65] J. F. Mendez-Valderrama and D. Chowdhury, *Phys. Rev. B* **103**, 195111 (2021).

[66] A. A. Patel, H. Guo, I. Esterlis, and S. Sachdev, [arXiv:2203.04990](https://arxiv.org/abs/2203.04990).

[67] H. v. Löhneysen, A. Rosch, M. Vojta, and P. Wölfle, *Rev. Mod. Phys.* **79**, 1015 (2007).

[68] S.-S. Lee, *Annu. Rev. Condens. Matter Phys.* **9**, 227 (2018).

[69] H.-C. Jiang, M. S. Block, R. V. Mishmash, J. R. Garrison, D. N. Sheng, O. I. Motrunich, and M. P. A. Fisher, *Nature (London)* **493**, 39 (2013).

[70] C. M. Varma, *Rev. Mod. Phys.* **92**, 031001 (2020).

[71] R. L. Smit, D. Valentini, J. Schmalian, and P. Kopietz, *Phys. Rev. Res.* **3**, 033089 (2021).

[72] L. Taillefer, *Annu. Rev. Condens. Matter Phys.* **1**, 51 (2010).

[73] R. Daou, O. Cyr-Choinière, F. Laliberté, D. LeBoeuf, N. Doiron-Leyraud, J.-Q. Yan, J.-S. Zhou, J. B. Goodenough, and L. Taillefer, *Phys. Rev. B* **79**, 180505(R) (2009).

[74] C. Yang, Y. Liu, Y. Wang, L. Feng, Q. He, J. Sun, Y. Tang, C. Wu, J. Xiong, W. Zhang, X. Lin, H. Yao, H. Liu, G. Fernandes, J. Xu, J. M. Valles, J. Wang, and Y. Li, *Science* **366**, 1505 (2019).

[75] K. S. Tikhonov and M. V. Feigel'man, *Ann. Phys. (Amsterdam)* **417**, 168138 (2020).